

# Geophysical Research Letters®

## RESEARCH LETTER

10.1029/2021GL094395

### Key Points:

- Aitken mode (20–60 nm) particles in the summertime high Arctic were composed of aged, organic-rich sea spray and secondary compounds
- An intense Aitken mode number increase was driven by the atmospheric breakup of pre-existing aerosol by an unknown mechanism

### Supporting Information:

Supporting Information may be found in the online version of this article.

### Correspondence to:

M. J. Lawler,  
[michael.lawler@colorado.edu](mailto:michael.lawler@colorado.edu)








### Citation:

Lawler, M. J., Saltzman, E. S., Karlsson, L., Zieger, P., Salter, M., Baccarini, A., et al. (2021). New insights into the composition and origins of ultrafine aerosol in the summertime high Arctic. *Geophysical Research Letters*, 48, e2021GL094395. <https://doi.org/10.1029/2021GL094395>

Received 29 JUN 2021

Accepted 18 OCT 2021

## New Insights Into the Composition and Origins of Ultrafine Aerosol in the Summertime High Arctic

M. J. Lawler<sup>1,2</sup> , E. S. Saltzman<sup>1</sup> , L. Karlsson<sup>3</sup>, P. Zieger<sup>3</sup> , M. Salter<sup>3</sup> , A. Baccarini<sup>4,5</sup> , J. Schmale<sup>5</sup> , and C. Leck<sup>6</sup> 

<sup>1</sup>Department of Earth System Science, Department of Chemistry, University of California, Irvine, Irvine, CA, USA, <sup>2</sup>Now at Cooperative Institute for Research in Environmental Science, CU Boulder, NOAA Earth System Research Laboratories, Boulder, CO, USA, <sup>3</sup>Department of Environmental Science, Stockholm University, Stockholm, Sweden, <sup>4</sup>Laboratory of Atmospheric Chemistry, Paul Scherrer Institute, Villigen, Switzerland, <sup>5</sup>Extreme Environments Research Laboratory, École Polytechnique Fédérale de Lausanne, Lausanne, Switzerland, <sup>6</sup>Department of Meteorology, Stockholm University, Stockholm, Sweden

**Abstract** The summertime high Arctic atmosphere is characterized by extremely low aerosol abundance, such that small natural aerosol inputs have a strong influence on cloud formation and surface temperature. The physical sources and the mechanisms responsible for aerosol formation and development in this climate-critical and changing region are still uncertain. We report time-resolved measurements of high Arctic Aitken mode (~20–60 nm diameter) aerosol composition during August–September 2018. During a significant Aitken mode formation event, the particles were composed of a combination of primary and secondary materials. These results highlight the importance of primary aerosol sources for high Arctic cloud formation, and they imply the action of a poorly understood atmospheric mechanism separating larger particles into multiple sub-particles.

**Plain Language Summary** Clouds are an important part of Earth's climate system, in part because they play a role in controlling how much energy passes from the sun to Earth's surface and from Earth's surface out into space. Aerosols, or disperse atmospheric particles, act as seeds onto which water can condense to form cloud droplets. The high Arctic region, near the North Pole, is a unique environment because it often has very low numbers of aerosols, which impacts the formation of clouds and their energy trapping and releasing properties. We set out to learn more about how aerosols form in this remote region, where climate is rapidly changing, with likely impacts on aerosol sources. We measured the composition of small, so-called ultrafine particles and found that they are made of a combination of sea spray and molecules added onto them as gases from the air. Surprisingly, it seems that sometimes large numbers of particles are formed from the breakup of larger composite particles, a process which has been hypothesized but, if it is occurring, is still not understood.

### 1. Introduction

Aerosol-cloud interactions have a significant effect on the energy budget of the summertime high Arctic (north of 80°). During the sunlit summer months, low clouds have a net warming effect on the atmospheric boundary layer (Tjernström et al., 2012). In cloud-free conditions, surface air temperatures are typically lower by several degrees. Isentropic atmospheric transport to the summertime high Arctic is limited by “domes” of low constant potential temperature, particularly at lower elevations (Klonecki et al., 2003; Stohl, 2006). In fog-forming and cloud-forming conditions, northward air transport at low levels occurs (Pithan et al., 2018), but these conditions lead to scavenging losses (Heintzenberg & Leck, 2012; Leck & Persson, 1996; Nilsson & Leck, 2002). As a result, the concentrations of transported continental aerosols and aerosol precursors are overall extremely low over the pack ice (Bigg et al., 2001; Chang et al., 2011; Kerminen & Leck, 2001). Local emissions of primary sea spray aerosols are also inhibited by the presence of sea ice, and pack ice sources of the sulfate precursor diethylsulfide (DMS) are negligible (Leck & Persson, 1996; Lundén et al., 2007; Nilsson & Leck, 2002). Aerosol concentrations in the summertime high Arctic are sometimes low enough to preclude cloud formation (Bigg et al., 1996; Mauritsen et al., 2011). Therefore, even relatively small natural sources of aerosol can have a significant impact on cloudiness,

surface temperature, and ice melt. There remains significant uncertainty about the composition and formation pathways of high Arctic aerosol.

Much of what is known about high Arctic summertime aerosols is based on a series of expeditions of the Swedish I/B *Oden* over the past three decades (Leck et al., 1996, 2001, 2004; Tjernström et al., 2014). These studies led to the remarkable findings that primary polymer gel particles from the surface ocean are an aerosol source and that some sea spray particles may be effectively sea salt-free (Bigg & Leck, 2008; Leck et al., 2002; Leck & Bigg, 2005b; Orellana et al., 2011). The gels found in boundary layer aerosol near the North Pole were similar to those found in the seawater in nearby open leads, consistent with a local primary sea spray source of the aerosol material (Orellana et al., 2011). This is surprising given that sea spray fluxes seem to be very low in the pack ice, where wind-driven wave breaking is strongly curtailed by the lack of long fetches of open water (Held et al., 2011; Norris et al., 2011).

One puzzling aerosol phenomenon observed in this region is the episodic appearance of sustained high concentrations of slowly growing or non-growing particles at sizes smaller than 100 nm diameter, generally appearing in two or three distinct size modes at once (Leck & Bigg, 1999). The particles have not been readily explained by local new particle formation from nucleation and growth originating from gas phase precursors, based on the size distribution dynamics and the low apparent contribution from secondary components like sulfuric acid (Karl et al., 2013; Leck & Bigg, 2010). This has led to speculation that these particles originate from the atmospheric breakup of larger aggregate aerosols, perhaps related to phase changes of aerosolized gels derived from the sea surface, but it has not yet been possible to test this hypothesis observationally (Karl et al., 2013; Leck & Bigg, 2010). High Arctic nanoparticle events, defined as a doubling of hourly averaged integrated particle number, represented 17% of the sample periods in the four previous expeditions (Karl et al., 2013). A consistent physical explanation or experimental demonstration of such a process is lacking, but fogs may play a role (Heintzenberg et al., 2006). Recent results have characterized frequent particle nucleation from iodic acid (Baccarini, Karlsson, et al., 2020), a compound that was not previously considered and which could play a role in the formation and composition of high Arctic Aitken mode aerosol.

Here, we report direct composition observations of the difficult-to-probe Aitken mode in the summertime high Arctic obtained as part of the international collaboration Microbiology Ocean Cloud Coupling in the High Arctic (MOCCHA), part of the Arctic Ocean 2018 (AO18) expedition. Observations were made using the Thermal Desorption Chemical Ionization Mass Spectrometer (TDCIMS), an instrument capable of broad chemical characterization of aerosols of 10s of nm diameter with sufficient time resolution to detect changes on timescales of a few hours. These observations are the first composition measurements of Arctic Aitken mode particles at such fine time resolution. They enable a detailed analysis of an intense particle formation event and provide new constraints on the possible formation pathways of these particles.

## 2. Materials and Methods

### 2.1. AO18 Expedition

The AO18 expedition included studies of aerosol processes, meteorology, and sea ice and open lead biogeochemistry with a major goal of identifying the sources and cloud-forming roles of aerosols linked to the microbial life in the ocean and ice north of 80° latitude. The main sampling period of the expedition was during a month-long ice camp from August 14 to September 14 during persistent daytime, when the icebreaker (I/B) *Oden* was moored to a large ice floe (Figures S1 and S2 in Supporting Information S1), and only data from this period are reported here. While at ice camp, the ship was periodically repositioned based on meteorological forecasts to secure a clean sampling wind sector for the instruments, which were mostly located forward on the fourth deck. Periods of contamination of sample air by the ship stack were identified using particle number concentrations and are excluded from further analysis. All times are reported as UTC.

### 2.2. Analyzing Aitken Mode Aerosol Composition With TDCIMS

The Thermal Desorption Chemical Ionization Mass Spectrometer (TDCIMS) is capable of size-selectively analyzing the aerosol composition of particles with diameters from about 10–200 nm (Lawler et al., 2018;

Voisin et al., 2003). During AO18, the TDCIMS sampled ambient air from a port on a shared ~1,100 liter per minute (LPM) inlet with a 10  $\mu\text{m}$  cutoff, identical to that used in previous expeditions (Leck et al., 1996, 2001). This 10  $\mu\text{m}$  inlet extended forward at a 45° angle from the top of a triple-wide instrument container affixed to the fourth deck on board *I/B Oden*. The top of the inlet was about 3 m above the surface of the container and about 25 m above the sea surface. The TDCIMS was run alternately in positive and negative ion modes with collection times of 30–120 min and calibrated for sodium, potassium, polysaccharide, ammonium, dimethylammonium, chloride, sulfate, methanesulfonate, and iodic acid. Most collections targeted aerosol of about 20–60 nm diameter. Mass fractions reported for these species are geometric means (GMs, reported with 0.25–0.75 quantiles) for period averages (details below). Period differences are considered statistically significant if their GMs have a probability  $p < 0.05$  of being equal. Details of the analysis are given in Text S1.1 in Supporting Information S1.

### 2.3. Additional Observations

The ambient aerosol size distribution was measured from 2 to 920 nm using a neutral air ion spectrometer (NAIS, Airel) on an independent short inlet and a custom differential mobility particle sizer (DMPS) using a mixing condensation particle counter (MCPC, Brechtel Manufacturing, Inc.) sampling on an independent whole air inlet (Baccarini et al., 2021; Baccarini, Karlsson, et al., 2020). An aerosol particle sizer (APS, TSI) on the whole air inlet was used to measure the size distribution of particles of >0.5–20  $\mu\text{m}$  diameter. The sampled particles were dried to about 12% RH by heating in the whole air inlet. Wind speed and direction were measured from a weather station installed on the forward mast of the *Oden*. Radiosondes were launched every 6 h to measure the vertical structure of the atmosphere. Five surface snow samples and two cloud water samples were collected and analyzed for major ions with ion chromatography and for polysaccharides using offline TDCIMS (see Text S1.3 in Supporting Information S1). Cloud water sampling is described in Zinke et al. (2021). A nitrate chemical ionization mass spectrometer (TOF-CIMS, Aerodyne Research, Inc.) was used to measure gas phase sulfuric acid ( $\text{H}_2\text{SO}_4$ ), methanesulfonic acid (MSA), and iodic acid ( $\text{HIO}_3$ ) (Baccarini, Schmale, et al., 2020). Four-day air mass back trajectories for air arriving at the surface at *Oden*'s position were calculated using LAGRANTO (Sprenger & Wernli, 2015).

## 3. Observational Results

### 3.1. Aitken Mode Dynamics

Concentrations of Aitken and accumulation mode particles were very low during the expedition. The median (0.25–0.75 quantile) concentration of 15–70 nm particles during the ice drift was 21 (8.9–51)  $\text{cm}^{-3}$  and for 70–1,000 nm particles was 13 (5.9–23.7)  $\text{cm}^{-3}$  based on DMPS measurements. From about August 30 to September 9, Aitken mode number concentrations were often several times higher than the accumulation mode. This period includes the most intense increase in Aitken mode number concentration observed during the ice drift, described in detail below. Around August 27, there was a shift to frequent iodine-driven particle nucleation and higher concentrations of Aitken mode particles (Baccarini, Karlsson, et al., 2020). This also roughly coincided with the onset of freezing of the sea surface (Vüllers et al., 2020). Therefore, we define drift period 1 (P1) as August 14–26 and drift period 2 (P2) as August 27 to September 14 for purposes of comparing aerosol composition under the different conditions. The occasional presence of fog may impact aerosol populations, causing some Aitken mode particles which have activated into droplets to be excluded from sampling by the 10  $\mu\text{m}$  cutoff inlet. Periods with surface visibility <2 km were characterized as fog periods and compared against non-fog periods.

### 3.2. Aitken Mode Mean Composition

Sulfate ( $\text{SO}_4^{2-}$ ) was detected in essentially all particle collections and represented 28 (18–43)% of the Aitken mode mass over the drift period, higher than any other species (Figure 1 and Table S1 in Supporting Information S1). Iodine, assumed to be in the form of iodic acid ( $\text{HIO}_3$ ), was also detected in essentially all samples due to very high instrumental sensitivity, but it represented on average only about 0.7 (0.26–2.0)% of the Aitken mode mass. Methanesulfonate (MSA,  $\text{CH}_3\text{SO}_3^-$ ) was similarly low in abundance. Polysaccharides

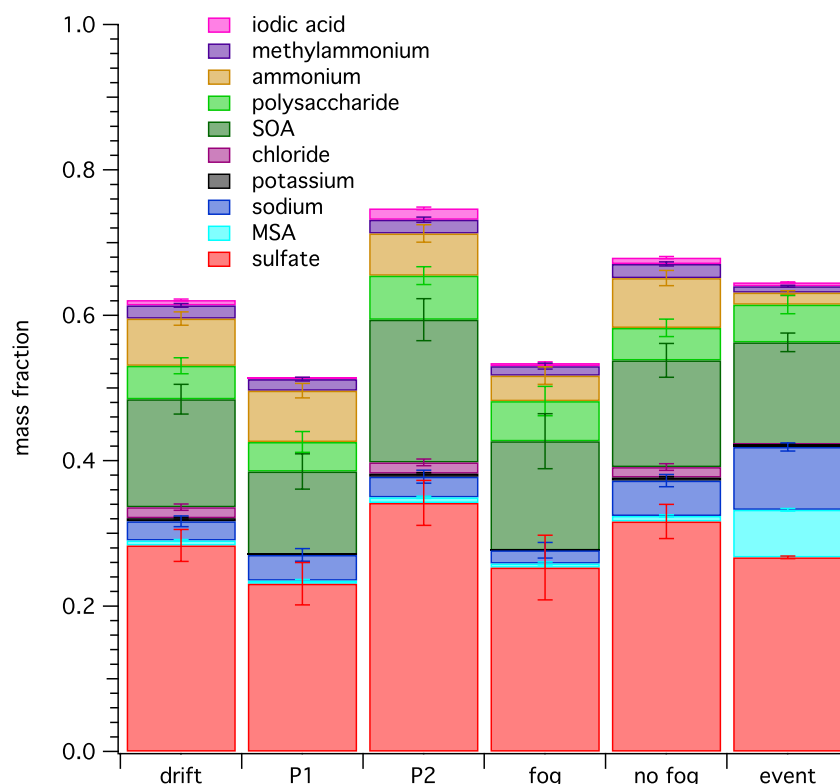


**Figure 1.** Geometric mean (GM) mass fractions of Aitken mode aerosol composition over the whole drift, P1, P2, foggy, and non-foggy periods, as well as the mass fractions taken for each ion mode at the most representative time point of the new Aitken mode formed during the August 30th event at the end of its stable growth period. For period averages, error bars are 1 standard deviation of the GM, and for the event data, error bars reflect ion counting error.

represented about 4.6 (1.6–14)%. Estimated SOA was 15 (8.8–25%). Ammonium ( $\text{NH}_4^+$ ) was about 6.5 (3.8–11)%, or a molar ratio to sulfate of 1.2, implying an average composition close to ammonium bisulfate, with only a minor molar contribution from methylammonium (MA,  $\text{CH}_3\text{NH}_3^+$ ), the most abundant and regularly detected amine. Sodium represented 2.6 (0.76–9.1)% of the mass on average, and chloride 1.5 (0.56–4.1)%. Chloride was very rarely detected in the Aitken mode, mostly during sea spray periods (notably September 12, Figure S3 in Supporting Information S1). That  $\text{Cl}^-:\text{Na}^+$  molar ratios were low indicates the usual volatilization of HCl during aging (Keene et al., 1998). On average, about half of the sampled Aitken mode mass could be quantified with calibrated species. The unaccounted-for mass likely includes compounds to which the TDCIMS is less sensitive, for example, non-polysaccharide primary marine organic aerosol (Lawler et al., 2020), but it could also partly arise from uncertainties in particle shape, density, and collection efficiency, or an overestimate of SOA sensitivity (see Text S1.1 in Supporting Information S1).

Most of the secondary species measured (with the exception of nitrogen bases) were present at statistically significantly higher mass fractions in P2 compared to P1: sulfate ( $p = 0.0010$ ), iodic acid ( $p = 3.9\text{e}-19$ ), MSA ( $p = 0.027$ ), and SOA ( $p = 0.0038$ ), with the largest fractional increases in sulfate (+48%), SOA (+71%), and iodic acid (+660%). No statistically significant differences in mass fraction for the primary species were identified. Part but not all of the difference between P1 and P2 may be due to the more frequent fogs in P1 (see Figure S3 in Supporting Information S1). Compounds that had statistically significantly lower mass fractions during fogs were sulfate ( $p = 0.026$ ), sodium ( $p = 0.0031$ ), methylamine ( $p = 0.029$ ), and iodic acid ( $p = 0.0070$ ). Sodium had a 63% lower mass fraction in fogs, alongside reductions in iodic acid (–51%), sulfate (–20%), and MA (–34%). Aitken mode particles with high mass fractions of hygroscopic sodium and sulfate salts may have preferentially activated into droplets and been either deposited to the sea surface or undersampled by the 10  $\mu\text{m}$  inlet. Iodic acid is not thought to be particularly hygroscopic (Murray et al., 2012), so its lower mass fraction in fogs could be due to a significant part of the aerosol iodine being nucleated particles which grew by sulfate addition and/or due to the fact that gas phase iodic

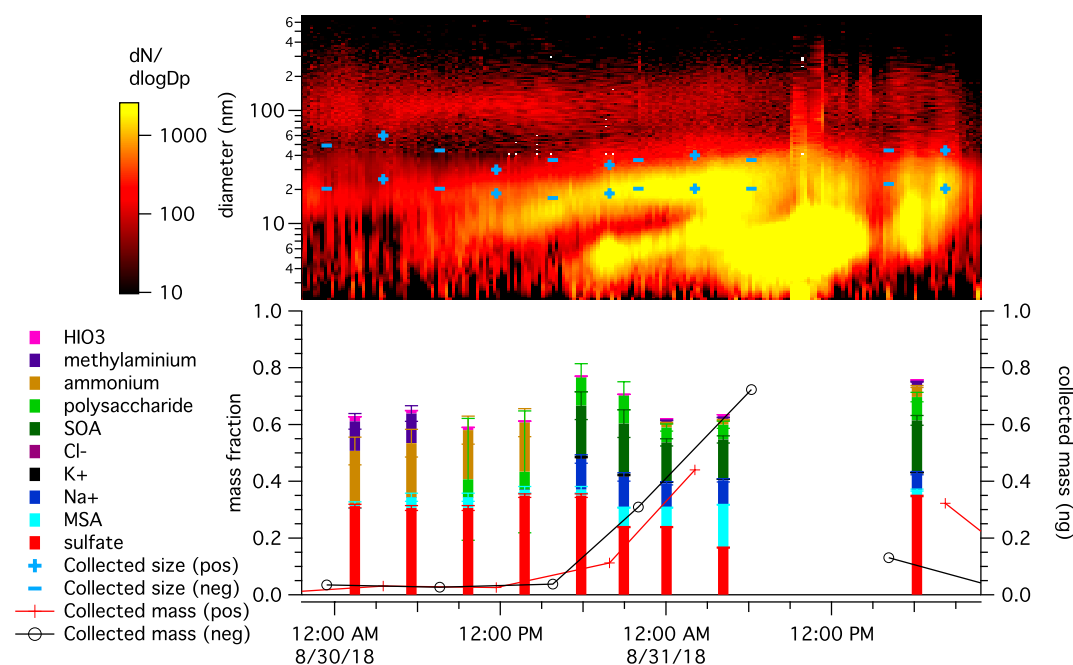


**Figure 2.** Upper plot: aerosol size distribution time series from merged NAIS and DMPS data. The blue crosses show the maximum and minimum particle diameters above and below which less than 5% of the sampled mass is contributed during each TDCIMS positive ion mode analysis, and blue horizontal lines show the same for TDCIMS negative ion analysis. Lower plot: combined positive and negative mode TDCIMS composition mass fractions for particles sampled during the August 30 event. Error bars are  $\pm$  one standard error and are only plotted for species that were detectable at a given time point.  $\text{Cl}^-$  is the only calibrated species presented here which was not detectable at any point during this time period. The gap in TDCIMS data on August 31st is due to contamination from ship stack as the wind shifted and the icebreaker was shifted to a new clean sampling orientation (note spikes in aerosol size distribution).

acid concentrations were lower in fogs, resulting in less iodic acid condensation onto particles (Baccarini, Karlsson, et al., 2020).

### 3.3. August 30 and 31 Aitken Mode Event

On August 30 and 31, there was an Aitken mode formation event during which a mode of particles around 10–20 nm diameter began to appear and increased in both number and diameter over several hours (Figures 2 and 3). Shortly after the appearance of this mode, a smaller mode centered around 5 nm also appeared. By around 22:00 August 30, significant increases in absolute ambient Aitken mode concentrations of sulfate, inorganic iodine, MSA, polysaccharide, potassium, and sodium were apparent (Figure S6 in Supporting Information S1). MSA was the only measured species that increased as a fraction of collected Aitken mode particle mass over the course of the event. This may be due both to an increase in the contribution from the new mode to the collected mass and/or to an actual change in the growing mode composition. Unfortunately, gas phase acid measurements were not available during the entire growth period of this event. Following the growth period, from 22:20 August 30 to 03:00 August 31,  $[\text{H}_2\text{SO}_4]$  was  $1.59 \pm 0.26 \times 10^5 \text{ molec cm}^{-3}$  and  $[\text{MSA}]$  was  $0.78 \pm 0.10 \times 10^5 \text{ molec cm}^{-3}$  (mean  $\pm$  std dev.).  $[\text{HIO}_3]$  was  $1.7 \pm 0.3 \times 10^6 \text{ molec cm}^{-3}$ , over an order of magnitude more abundant than either sulfur gas. The event occurred coincident with cloud breakup and very high surface visibility (Figure S6 in Supporting Information S1). The highest mass fractions and absolute air concentrations of Aitken mode MSA for the entire drift period were measured during this event. The event also had the highest absolute air concentrations of sodium and potassium in the Aitken mode measured during this expedition, higher even than during high wind sea spray events during P2.

To better characterize the particle dynamics over this period, the merged aerosol size distribution was averaged over 1 h periods and fitted with five log-normal distributions (Figures 3, S7, and S8 in Supporting Information S1). There was one coherent mode that contributed to the increases in Aitken mode particle

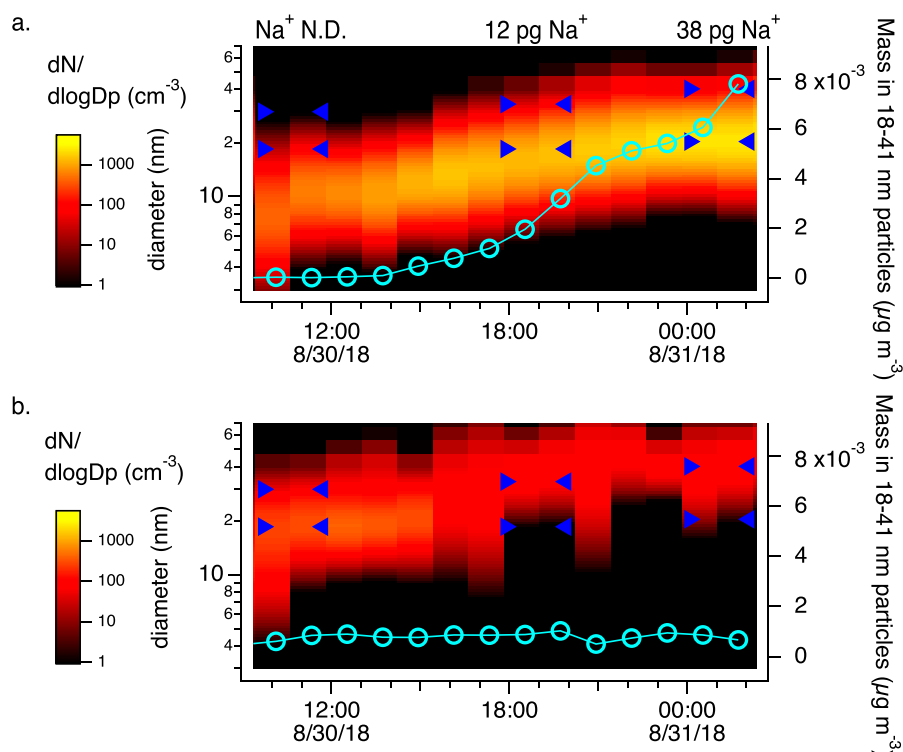


**Figure 3.** Decomposition of the ambient 10–70 nm particles during the August 30th event into two log-normal modes, a newly appearing mode (a) and a pre-existing mode (b). Light blue circles indicate the mass present from each mode in 18–41 nm particles, the range of particle sizes collected during the event. Dark blue triangles in groups of 4 encompass the particle size ranges and time range of 3 collections analyzed in TDCIMS positive ion mode. The pre-existing mode at 20 nm was well-resolved until about 16:00, after which the new mode overlapped and the algorithm only found another low concentration mode at a slightly larger diameter, which also did not contribute appreciably to the mass collected when sodium was detected in the particles. Absolute collected mass of Na<sup>+</sup> in pg is given above each collection period shown.

collected mass and signal during a period with stable wind direction and trace gases from about 09:00 August 30 to 02:00 August 31 (Figures S6 and S9 in Supporting Information S1). This mode appeared at a modal diameter of roughly 10 nm at around 50 particles  $\text{cm}^{-3}$  and increased to a modal diameter of about 20 nm and a concentration of about 700 particles  $\text{cm}^{-3}$  (Figures 3 and S8 in Supporting Information S1). The pre-existing aerosol present in the TDCIMS sampling diameter range (about 18–41 nm over this period) contributed only a small amount of sampled mass once the new particles reached collectable sizes. As these new particles increased in number and mass, essentially all detected species increased in abundance, including primary species like sodium (Figures 3 and S6 in Supporting Information S1).

#### 4. Possible Aitken Mode Formation Mechanisms in the Event

The composition measurements reported above place strong constraints on the possible mechanisms for the formation of the Aitken mode during Aitken mode number enhancement events in the summertime high Arctic, and for summertime high Arctic Aitken aerosol more generally. The overall composition of the event particles was similar to that over the drift period, despite much higher concentrations during the event. This suggests that the processes that form the event particles may also be important for the “background” Aitken mode aerosol.

The August 30th event is hard to interpret in terms of well-understood aerosol processes. The sodium, potassium, and apparent polysaccharides in the newly formed mode are clear evidence against a sole gas-to-particle conversion origin. While there was clear evidence for newly formed particles in the <10 nm nucleation mode, most likely driven by iodine chemistry (Baccarini, Karlsson, et al., 2020), the Aitken mode

composition was not consistent with iodic acid growth or coagulation of iodic acid particles being a major source of Aitken mode mass. Growth from gas phase sulfuric and/or methanesulfonic acids at concentrations measured in situ (several times lower than iodic acid) could also not explain the rapid growth ( $>1 \text{ nm hr}^{-1}$ ) of this event (Baccarini, Karlsson, et al., 2020). These considerations indicate that most of the growth probably occurred upwind of the sampling location under conditions of higher MSA and sulfuric acid gas phase concentrations, presumably closer to larger dimethylsulfide sources at the marginal ice zone in more open water. Such spatiotemporal inhomogeneities in particle formation and growth can result in size distribution dynamics such as we observed, with local observed increases in particle diameter driven by growth that occurred upwind (Kivekäs et al., 2016, Figure 4).

We consider below three broad hypotheses for the formation of the Aitken mode particles during the August 30th event: (a) “blowing snow,” i.e., saltation of snow from the sea ice surface followed by sublimation, (b) “sea spray aging,” i.e., sea spray, possibly generated in low-ice conditions further south, and aged in transit, and (c) “sea spray aging and breakup,” i.e., the formation of many small particles from larger aged organic-rich primary particles in the atmosphere.

#### 4.1. Blowing Snow Hypothesis

The formation of Aitken mode aerosols from evaporation of blowing snow is unlikely to explain the field observations. Snow samples collected during the campaign show much lower polysaccharide/ $\text{Na}^+$  ratios than were observed in Aitken mode aerosol (Figure S12 in Supporting Information S1). Very fresh snow showed the highest ratio, but it was still several times lower than typical for the Aitken mode. In addition, the  $\text{Na}^+$  concentration in snow was high enough that to make a 30-nm diameter particle with 10%  $\text{Na}^+$  by mass, a sublimating snow particle would have to be less than  $2 \mu\text{m}$  original diameter. Blowing snow is typically 1–2 orders of magnitude larger (Gordon & Taylor, 2009; Yang et al., 2019), so the simultaneous presence of much larger particles would be expected. Furthermore, APS observations showed maximum of  $0.5\text{--}20 \mu\text{m}$  particle concentrations before the event less than  $1 \text{ cm}^{-3}$ , much too low to contribute appreciably to the  $100 \text{ s cm}^{-3}$  Aitken mode concentrations. In the present case particles larger than  $\sim 70 \text{ nm}$  actually decreased slightly in number as Aitken mode number increased (Figure S13 in Supporting Information S1).

#### 4.2. Sea Spray Aging Hypothesis

There is considerable evidence against local (in the pack ice) primary sea spray aerosols as the source of Aitken mode aerosol observed. Observations during the present expedition from a primary aerosol flux chamber and subsurface bubble camera deployed at the open lead site showed that for most of the time, bubble bursting and primary aerosol formation were negligible. During a strong wind event on September 12th, when winds were above  $10 \text{ m s}^{-1}$  for about 15 hr, appreciable numbers of sea spray particles were formed. Even during this relatively intense event, the concentration of  $15\text{--}50 \text{ nm}$  diameter particles was almost a factor of 10 lower than during the sustained Aitken mode event on August 30 and 31, and the absolute concentration of sodium in the Aitken mode was about eight times lower. In addition, the sulfate-dominated aging of the particles is not consistent with the local iodine-dominated gas phase condensable acids observed.

Similarly, sea spray transported from the marginal ice zone or from open waters south of the pack ice would provide too small a number flux to explain the August 30th event. The particles increased in number over 10 h at a rate of  $34 \text{ cm}^{-3} \text{ hr}^{-1}$  (Figure S8 in Supporting Information S1). They were first detected at a modal diameter of about  $10 \text{ nm}$ . Over this period the atmospheric surface mixed layer depth gradually decreased to a minimum of about  $180 \text{ m}$ . Given that mixing depth, a  $10 \text{ m s}^{-1}$  wind speed, and a  $273\text{K}$  sea surface temperature, the total rate of new sea spray particles of  $1\text{--}20 \text{ nm}$  diameter is estimated at about  $0.2 \text{ cm}^{-3} \text{ hr}^{-1}$  (Salter et al., 2015), over  $100\times$  too low. If an increasing sea spray flux were combined with a coincident increasing nucleation flux to produce the observed mode, the ultrafine sea spray flux would still need to provide about 25% of the number flux, or  $25\times$  higher than estimated from the sea spray source function (See Text S1.6 in Supporting Information S1). Even if there could be a sufficiently large source, these sea spray hypotheses would require the rapid loss of all sea spray formed at  $> 50 \text{ nm}$  sizes ( $>80\%$  of the number flux) since the accumulation mode aerosol number concentration actually decreased over this period (Figure S13

in Supporting Information S1). Since some fraction of primary accumulation mode particles clearly remain after formation based on the regular observation of  $\text{Na}^+$  in the accumulation mode (Figure S14 in Supporting Information S1), it seems unlikely that a several-fold increase in primary Aitken mode-sized particles would be accompanied by a modest decrease in accumulation mode particles if sea spray were the source.

### 4.3. Primary Aerosol Transport, Aging, and Breakup Hypotheses

A more controversial hypothesis to explain the August 30th event is that high Arctic Aitken mode particles were formed from the breakup of larger particles or droplets (Figure S15 in Supporting Information S1). It has been proposed that primary marine gel particles present in droplets change phase to a collapsed nanoparticle state, potentially driven by a decrease in pH and/or photochemical degradation of the gel polymers (Karl et al., 2013). These processes are well-understood for marine gels dispersed in seawater (Orellana & Leck, 2015) and are likely to occur in the Arctic aerosols and droplets as they photochemically age in the atmosphere. Agglomerations of nanoparticles have been observed in high Arctic aerosols, clouds, and sea surface microlayer and linked to marine gels (Bigg et al., 2004; Karl et al., 2013; Leck & Bigg, 2005a; Orellana et al., 2011), but a mechanism for subsequent aggregate breakup in the atmosphere has never been determined. Charge buildup alone probably does not suffice (Leck & Bigg, 2010). Shear forces require air velocities on the order of  $100 \text{ m s}^{-1}$  to measurably break up accumulation mode agglomerates (Ding et al., 2016). Steric repulsion of nanoparticles with polysaccharide chains and electrostatic repulsion of negative functional groups (typical in marine gels) can hinder aggregation in dispersions (Adroher-Benítez et al., 2017; Bachhar & Bandyopadhyaya, 2016; Moncho-Jordá, 2013). However, it is not clear that the sum of such repulsive forces could suffice to separate nanoparticles from aggregates or evaporating droplets in the atmosphere, or at what rates this might occur. To achieve  $34 \text{ cm}^{-3} \text{ hr}^{-1}$  formation of 15 nm particles would only require  $0.11 \text{ cm}^{-3} \text{ hr}^{-1}$  loss of 100 nm particles assuming complete mass transfer, such that losses in accumulation mode particle number would be difficult to detect. The same chemical species identified in the Aitken mode were also present in accumulation mode particles at broadly similar fractions during much of the drift, with statistically indistinguishable polysaccharide:sodium ratios (Figures S14 and S12 in Supporting Information S1), making them a compositionally plausible source.

One demonstrated pathway to forming many smaller droplets or particles from one parent droplet is secondary ice formation (Field et al., 2016; Hallett & Mossop, 1974). Upon subsequent evaporation or sublimation, the resultant ice fragments could each leave behind a smaller particle if the non-water components are distributed throughout the ice particle. The estimated rates of secondary ice formation vary over orders of magnitude but overall are likely too slow to explain the present observations (Fu et al., 2019; Hobbs & Rangno, 1990). However, recent laboratory results indicate that jetting and bubble bursting can accompany droplet freezing and appear to generate large numbers of liquid particles (Keinert et al., 2020; Lauber et al., 2018). Submicron particles were not measured in these studies, but they strongly imply the existence of a mechanism by which one hydrometeor could generate many smaller droplets that could lead to aerosol upon evaporation.

In any case, the high mass fractions of secondary compounds imply a significant role for atmospheric aging in Aitken mode growth and overall composition during the event and throughout the drift period. Considering the Aitken mode mass fractions at the end of the event's stable growth period, polysaccharide is estimated at 5.2% of particle mass and sodium at 8.6%, or roughly 14% primary material. An atmospherically aged sea spray-derived nanoparticle made of polysaccharide and sodium plus sulfate for charge balance freed by some process from a larger aggregate or droplet at a dry diameter of 15 nm and grown by gas addition to a dry diameter of 25 nm would be 11% "primary" volume. This is roughly consistent with measured composition and the development of the aerosol size distribution in the event. Given the iodic acid mass fraction of the event particles, the growth rate as measured by Baccarini, Schmale, & Dommen (2020) of  $1.2 \text{ nm hr}^{-1}$ , and the iodic acid gas phase concentration at the end of the event, iodic acid could have contributed to about 3% of the growth if present at comparable levels upwind (Nieminen et al., 2010). Iodic acid represented about 1% of the secondary aerosol mass of the particles, roughly consistent with the estimated modest contribution by condensational growth of iodic acid. In contrast, MSA contributed substantially to the growth, consistent with previous studies linking ultrafine Arctic aerosol formation and growth events to enhanced



atmospheric MSA levels (Heintzenberg & Leck, 1994; Willis et al., 2016), showing the likely importance of biogenic emissions for such events.

## 5. Conclusions

Observations of ultrafine aerosol size, number, and composition provide new insights into the drivers of aerosol composition and formation events in the summertime high Arctic. Seawater cations, secondary sulfate, methanesulfonate, iodic acid, secondary organic aerosol, and polysaccharide-like organics all contributed to Aitken mode composition during an intense formation event, and these species were found in similar fractional abundances in the Aitken mode throughout the summer to fall transition period of the observations. The event was not consistent with primary aerosol emission and well-understood atmospheric aging processes, or with nucleation from gaseous precursors. The breakup of larger particles, presumably marine gel-derived aggregates, remains an unproven but viable hypothesis for this and other similar, previously reported high Arctic events. Whatever the mechanisms involved, it appears that there exists a pathway for the processing and “recycling” of transported sea spray in the extremely aerosol source-limited high Arctic, possibly representing a significant CCN source in this region. To elucidate these mechanisms and better constrain Arctic aerosol-cloud interactions, laboratory and numerical studies investigating aerosol formed from droplet freezing and the dynamics of charged nanoparticles in evaporating droplets are needed.

## Conflict of Interest

The authors declare no conflicts of interest relevant to this study.

## Data Availability Statement

All data are available at the Bolin Data Centre ([bolin.su.se/data/](http://bolin.su.se/data/)) with keyword MOCCHA.

## Acknowledgments

The Swedish Polar Research Secretariat (SPRS) provided access to the I/B *Oden* and logistical support in collaboration with the U.S. National Science Foundation. The authors are grateful to co-Chief Scientist Patricia Matrai for planning, technical support, and coordination of AO2018, to the SPRS logistical staff and to I/B *Oden*'s Captain Mattias Peterson and his crew for expert field support. This work was supported by the National Science Foundation Arctic Natural Sciences program (Grant 1738629), Swiss National Science Foundation (Grant no. 200021\_169090), the Swiss Polar Institute, the BNP Paribas Swiss Foundation (Polar Access Fund 2018), the Knut and Alice Wallenberg Foundation within the ACAS project (Arctic Climate Across Scales, Project no. 2016.0024), the Bolin Centre for Climate Research (RA2), and the Swedish Research Council (Project nos. 2018-05045, 2016-03518, and 2016-05100). J.S. holds the Ingvar Kamprad Chair, sponsored by Ferring Pharmaceuticals. The authors thank the AO18 ice core team for retrieving surface snow samples and Julika Zinke (University of Stockholm) for provision of cloud water samples. The authors also thank Heini Wernli (ETH Zürich, Switzerland) for calculating the air mass back trajectories, John Prytherch (Stockholm University, Sweden) for processing meteorological data, and Jutta Villers (University of Leeds) for useful meteorological discussions.

## References

- Adroher-Benítez, I., Martín-Molina, A., Ahualli, S., Quesada-Pérez, M., Odriozola, G., & Moncho-Jordá, A. (2017). Competition between excluded-volume and electrostatic interactions for nanogel swelling: Effects of the counterion valence and nanogel charge. *Physical Chemistry Chemical Physics*, 19(9), 6838–6848. <https://doi.org/10.1039/c6cp08683g>
- Baccarini, A., Karlsson, L., Dommen, J., Duplessis, P., Villers, J., Brooks, I. M., et al. (2020). Frequent new particle formation over the high Arctic pack ice by enhanced iodine emissions. *Nature Communications*, 11(1), 1–11. <https://doi.org/10.1038/s41467-020-18551-0>
- Baccarini, A., Schmale, J., & Dommen, J. (2020). Iodic acid, sulfuric acid and methanesulfonic acid collected during the Arctic Ocean 2018 expedition. <https://doi.org/10.17043/ao2018-aerosol-cims>
- Baccarini, A., Schmale, J., Dommen, J., Karlsson, L., & Zieger, P. (2021). Size distribution of aerosol particles between 2.5 and 920 nm measured during the Arctic Ocean 2018 expedition. <https://doi.org/10.17043/ao2018-aerosol-merged-psd>
- Bachhar, N., & Bandyopadhyaya, R. (2016). Predicting complete size distribution of nanoparticles based on interparticle potential: Experiments and simulation. *Journal of Physical Chemistry C*, 120(8), 4612–4622. <https://doi.org/10.1021/acs.jpcc.5b11285>
- Bigg, E. K., & Leck, C. (2008). The composition of fragments of bubbles bursting at the ocean surface. *Journal of Geophysical Research*, 113(D11), D11209. <https://doi.org/10.1029/2007JD009078>
- Bigg, E. K., Leck, C., & Nilsson, D. E. (1996). Sudden changes in arctic atmospheric aerosol concentrations during summer and autumn. *Tellus B: Chemical and Physical Meteorology*, 48(2), 254–271. <https://doi.org/10.3402/tellusb.v48i2.15890>
- Bigg, E. K., Leck, C., & Nilsson, E. D. (2001). Sudden changes in aerosol and gas concentrations in the central Arctic marine boundary layer: Causes and consequences. *Journal of Geophysical Research*, 106(D23), 32167–32185. <https://doi.org/10.1029/2000JD900753>
- Bigg, E. K., Leck, C., & Tranvik, L. (2004). Particulates of the surface microlayer of open water in the central Arctic Ocean in summer. *Marine Chemistry*, 91(1–4), 131–141. <https://doi.org/10.1016/j.marchem.2004.06.005>
- Chang, R. Y. W., Leck, C., Graus, M., Müller, M., Paatero, J., Burkhart, J. F., et al. (2011). Aerosol composition and sources in the central Arctic Ocean during ASCOS. *Atmospheric Chemistry and Physics*, 11(20), 10619–10636. <https://doi.org/10.5194/acp-11-10619-2011>
- Ding, Y., Stahlmecke, B., Kaminski, H., Jiang, Y., Kuhlbusch, T. A. J., & Riediker, M. (2016). Deagglomeration testing of airborne nanoparticle agglomerates: Stability analysis under varied aerodynamic shield and relative humidity conditions. *Aerosol Science and Technology*, 50(11), 1253–1263. <https://doi.org/10.1080/02786826.2016.1216072>
- Field, P. R., Lawson, R. P., Brown, P. R. A., Lloyd, G., Westbrook, C., Moiseev, D., et al. (2016). Chapter 7. Secondary ice production—Current state of the science and recommendations for the future. *Meteorological Monographs*, 58(1), 7.1–7.20. <https://doi.org/10.1175/amsmonographs-d-16-0014.1>
- Fu, S., Deng, X., Shupe, M. D., & Xue, H. (2019). A modelling study of the continuous ice formation in an autumnal Arctic mixed-phase cloud case. *Atmospheric Research*, 228, 77–85. <https://doi.org/10.1016/j.atmosres.2019.05.021>
- Gordon, M., & Taylor, P. A. (2009). Measurements of blowing snow, Part I: Particle shape, size distribution, velocity, and number flux at Churchill, Manitoba, Canada. *Cold Regions Science and Technology*, 55(1), 63–74. <https://doi.org/10.1016/j.coldregions.2008.05.001>
- Hallett, J., & Mossop, S. C. (1974). Production of secondary ice particles during the growth of graupel by riming. *Nature*, 249, 27–57. <https://doi.org/10.1002/qj.49710243104>

- Heintzenberg, J., & Leck, C. (1994). Seasonal variation of the atmospheric aerosol near the top of the marine boundary layer over Spitsbergen related to the Arctic sulfur cycle. *Tellus*, *46B*, 52–67. <https://doi.org/10.1034/j.1600-0889.1994.00005.x>
- Heintzenberg, J., & Leck, C. (2012). The summer aerosol in the central Arctic 1991–2008: Did it change or not? *Atmospheric Chemistry and Physics*, *12*(9), 3969–3983. <https://doi.org/10.5194/acp-12-3969-2012>
- Heintzenberg, J., Leck, C., Birmili, W., Wehner, B., Tjernström, M., & Wiedensohler, A. (2006). Aerosol number-size distributions during clear and fog periods in the summer high Arctic: 1991, 1996 and 2001. *Tellus Series B Chemical and Physical Meteorology*, *58*(1), 41–50. <https://doi.org/10.1111/j.1600-0889.2005.00171.x>
- Held, A., Brooks, I. M., Leck, C., & Tjernström, M. (2011). On the potential contribution of open lead particle emissions to the central Arctic aerosol concentration. *Atmospheric Chemistry and Physics*, *11*(7), 3093–3105. <https://doi.org/10.5194/acp-11-3093-2011>
- Hobbs, P. V., & Rangno, A. L. (1990). Rapid development of high ice particle concentrations in small polar maritime cumuliform clouds. *Journal of the Atmospheric Sciences*, *47*(22), 2710–2722. [https://doi.org/10.1175/1520-0469\(1990\)047<2710:rdohip>2.0.co;2](https://doi.org/10.1175/1520-0469(1990)047<2710:rdohip>2.0.co;2)
- Karl, M., Leck, C., Coz, E., & Heintzenberg, J. (2013). Marine nanogels as a source of atmospheric nanoparticles in the high Arctic. *Geophysical Research Letters*, *40*(14), 3738–3743. <https://doi.org/10.1002/grl.50661>
- Keene, W. C., Sander, R., Pszenny, A. A. P., Vogt, T. R., Crutzen, P. J., Galloway, J. N., et al. (1998). Aerosol pH in the marine boundary layer: A review and model evaluation. *Journal of Aerosol Science*, *29*(3), 339–356. [https://doi.org/10.1016/S0021-8502\(97\)10011-8](https://doi.org/10.1016/S0021-8502(97)10011-8)
- Keinert, A., Spannagel, D., Leisner, T., & Kiselev, A. (2020). Secondary ice production upon freezing of freely falling drizzle droplets. *Journal of the Atmospheric Sciences*, *77*(8), 2959–2967. <https://doi.org/10.1175/JAS-D-20-0081.1>
- Kerminen, V. M., & Leck, C. (2001). Sulfur chemistry over the central Arctic Ocean during the summer: Gas-to-particle transformation. *Journal of Geophysical Research: Atmospheres*, *106*(D23), 32087–32099. <https://doi.org/10.1029/2000JD900604>
- Kivekäs, N., Carpman, J., Roldin, P., Leppä, J., O'Connor, E., Kristensson, A., & Asmi, E. (2016). Coupling an aerosol box model with one-dimensional flow: A tool for understanding observations of new particle formation events. *Tellus Series B: Chemical and Physical Meteorology*, *68*(1), 1–14. <https://doi.org/10.3402/tellusb.v68.29706>
- Klonecki, A., Hess, P., Emmons, L., Smith, L., Orlando, J., & Blake, D. (2003). Seasonal changes in the transport of pollutants into the Arctic troposphere-model study. *Journal of Geophysical Research*, *108*(4). <https://doi.org/10.1029/2002jd002199>
- Laubner, A., Kiselev, A., Pander, T., Handmann, P., & Leisner, T. (2018). Secondary ice formation during freezing of levitated droplets. *Journal of the Atmospheric Sciences*, *75*(8), 2815–2826. <https://doi.org/10.1175/JAS-D-18-0052.1>
- Lawler, M. J., Lewis, S., Russell, L. M., Quinn, P. K., Bates, T. S., Coffman, D. J., et al. (2020). North Atlantic marine organic aerosol characterized by novel offline thermal desorption mass spectrometry: Polysaccharides, recalcitrant material, and secondary organics. *Atmospheric Chemistry and Physics*, *20*(24), 16007–16022. <https://doi.org/10.5194/acp-2020-562>
- Lawler, M. J., Rissanen, M. P., Ehn, M., Lee Mauldin, R., III, Sarnela, N., Sipilä, M., & Smith, J. N. (2018). Evidence for diverse biogeochemical drivers of boreal forest new particle formation. *Geophysical Research Letters*, *45*, 2038–2046. <https://doi.org/10.1002/2017GL076394>
- Leck, C., & Bigg, E. K. (1999). Aerosol production over remote marine areas—A new route. *Geophysical Research Letters*, *26*(23), 3577–3580. <https://doi.org/10.1029/1999gl010807>
- Leck, C., & Bigg, E. K. (2005a). Biogenic particles in the surface microlayer and overlaying atmosphere in the central Arctic Ocean during summer. *Tellus Series B: Chemical and Physical Meteorology*, *57*(4), 305–316. <https://doi.org/10.1111/j.1600-0889.2005.00148.x>
- Leck, C., & Bigg, E. K. (2005b). Source and evolution of the marine aerosol—A new perspective. *Geophysical Research Letters*, *32*(19), L19803. <https://doi.org/10.1029/2005GL023651>
- Leck, C., & Bigg, E. K. (2010). New particle formation of marine biological origin. *Aerosol Science and Technology*, *44*, 570–577. <https://doi.org/10.1080/02786826.2010.481222>
- Leck, C., Bigg, E. K., Covert, D. S., Heintzenberg, J., Maenhaut, W., Nilsson, E. D., & Wiedensohler, A. (1996). Overview of the atmospheric research program during the International Arctic Ocean Expedition of 1991 (IAOE-91) and its scientific results. *Tellus Series B: Chemical and Physical Meteorology*, *48*(2), 136–155. <https://doi.org/10.3402/tellusb.v48i2.15833>
- Leck, C., Nilsson, E. D., Bigg, E. K., & Bäcklin, L. (2001). Atmospheric program on the Arctic Ocean Expedition 1996 (AOE-96): An overview of scientific goals, experimental approach, and instrumentation. *Journal of Geophysical Research*, *106*, 32051–32067. <https://doi.org/10.1029/2000jd900461>
- Leck, C., Norman, M., Bigg, E. K., & Hillamo, R. (2002). Chemical composition and sources of the high Arctic aerosol relevant for cloud formation. *Journal of Geophysical Research*, *107*(D12), 4135. <https://doi.org/10.1029/2001JD001463>
- Leck, C., & Persson, C. (1996). Seasonal and short-term variability in dimethyl sulfide, sulfur dioxide and biogenic sulfur and sea salt aerosol particles in the arctic marine boundary layer during summer and autumn. *Tellus Series B: Chemical and Physical Meteorology*, *48*(2), 272–299. <https://doi.org/10.3402/tellusb.v48i2.15891>
- Leck, C., Tjernström, M., Matrai, P., Swietucki, E., & Bigg, E. K. (2004). Can marine micro-organisms influence melting of the arctic pack ice? *Eos, Transactions, American Geophysical Union*, *85*(3), 25. <https://doi.org/10.1029/2004EO030001>
- Lundén, J., Svensson, G., & Leck, C. (2007). Influence of meteorological processes on the spatial and temporal variability of atmospheric dimethyl sulfide in the high Arctic summer. *Journal of Geophysical Research*, *112*(13), 1–17. <https://doi.org/10.1029/2006JD008183>
- Mauritsen, T., Sedlar, J., Tjernström, M., Leck, C., Martin, M., Shupe, M., et al. (2011). An Arctic CCN-limited cloud-aerosol regime. *Atmospheric Chemistry and Physics*, *11*(1), 165–173. <https://doi.org/10.5194/acp-11-165-2011>
- Moncho-Jordá, A. (2013). Effective charge of ionic microgel particles in the swollen and collapsed states: The role of the steric microgel-ion repulsion. *The Journal of Chemical Physics*, *139*(6), 064906. <https://doi.org/10.1063/1.4817852>
- Murray, B. J., Haddrell, A. E., Peppe, S., Davies, J. F., Reid, J. P., O'Sullivan, D., et al. (2012). Glass formation and unusual hygroscopic growth of iodine acid solution droplets with relevance for iodine mediated particle formation in the marine boundary layer. *Atmospheric Chemistry and Physics*, *12*(18), 8575–8587. <https://doi.org/10.5194/acp-12-8575-2012>
- Nieminen, T., Lehtinen, K. E. J., & Kulmala, M. (2010). Sub-10 nm particle growth by vapor condensation-effects of vapor molecule size and particle thermal speed. *Atmospheric Chemistry and Physics*, *10*(20), 9773–9779. <https://doi.org/10.5194/acp-10-9773-2010>
- Nilsson, E. D., & Leck, C. (2002). A pseudo-Lagrangian study of the sulfur budget in the remote Arctic marine boundary layer. *Tellus B: Chemical and Physical Meteorology*, *54*(3), 213–230. <https://doi.org/10.3402/tellusb.v54i3.16662>
- Norris, S. J., Brooks, I. M., De Leeuw, G., Sirevaag, A., Leck, C., Brooks, B. J., et al. (2011). Measurements of bubble size spectra within leads in the Arctic summer pack ice. *Ocean Science*, *7*(1), 129–139. <https://doi.org/10.5194/os-7-129-2011>
- Orellana, M. V., & Leck, C. (2015). Chapter 9—Marine microgels. In *Biogeochemistry of marine dissolved organic matter* (2nd ed.).
- Orellana, M. V., Matrai, P. A., Leck, C., Rauschenberg, C. D., Lee, A. M., & Coz, E. (2011). Marine microgels as a source of cloud condensation nuclei in the high Arctic. *Proceedings of the National Academy of Sciences of the United States of America*, *108*(33), 13612–13617. <https://doi.org/10.1073/pnas.1102457108>

- Pithan, F., Svensson, G., Caballero, R., Chechin, D., Cronin, T. W., Ekman, A. M. L., et al. (2018). Role of air-mass transformations in exchange between the Arctic and mid-latitudes. *Nature Geoscience*, *11*(11), 805–812. <https://doi.org/10.1038/s41561-018-0234-1>
- Salter, M. E., Zieger, P., Acosta Navarro, J. C., Grythe, H., Kirkevåg, A., Rosati, B., et al. (2015). An empirically derived inorganic sea spray source function incorporating sea surface temperature. *Atmospheric Chemistry and Physics*, *15*(19), 11047–11066. <https://doi.org/10.5194/acp-15-11047-2015>
- Sprenger, M., & Wernli, H. (2015). The LAGRANTO Lagrangian analysis tool—Version 2.0. *Geoscientific Model Development*, *8*(8), 2569–2586. <https://doi.org/10.5194/gmd-8-2569-2015>
- Stohl, A. (2006). Characteristics of atmospheric transport into the Arctic troposphere. *Journal of Geophysical Research: Atmospheres*, *111*(11), 1–17. <https://doi.org/10.1029/2005JD006888>
- Tjernström, M., Birch, C. E., Brooks, I. M., Shupe, M. D., Persson, P. O. G., Sedlar, J., et al. (2012). Meteorological conditions in the central Arctic summer during the Arctic Summer Cloud Ocean Study (ASCOS). *Atmospheric Chemistry and Physics*, *12*(15), 6863–6889. <https://doi.org/10.5194/acp-12-6863-2012>
- Tjernström, M., Leck, C., Birch, C. E., Bottenheim, J. W., Brooks, B. J., Brooks, I. M., et al. (2014). The Arctic Summer Cloud Ocean Study (ASCOS): Overview and experimental design. *Atmospheric Chemistry and Physics*, *14*(6), 2823–2869. <https://doi.org/10.5194/acp-14-2823-2014>
- Voisin, D., Smith, J., Sakurai, H., McMurry, P., & Eisele, F. (2003). Thermal desorption chemical ionization mass spectrometer for ultrafine particle chemical composition. *Aerosol Science and Technology*, *37*, 471–475. <https://doi.org/10.1080/02786820390125232>
- Vüllers, J., Achtert, P., Brooks, I., Tjernström, M., Prytherch, J., & Neely, R., III (2020). Meteorological and cloud conditions during the Arctic Ocean 2018 expedition. *Atmospheric Chemistry and Physics*, 1–43. <https://doi.org/10.5194/acp-2020-219>
- Willis, M. D., Burkart, J., Thomas, J. L., Köllner, F., Schneider, J., Bozem, H., et al. (2016). Growth of nucleation mode particles in the summertime Arctic: A case study. *Atmospheric Chemistry and Physics*, *16*(12), 7663–7679. <https://doi.org/10.5194/acp-16-7663-2016>
- Yang, X., Frey, M. M., Rhodes, R. H., Norris, S. J., Brooks, I. M., Anderson, P. S., et al. (2019). Sea salt aerosol production via sublimating wind-blown saline snow particles over sea ice: Parameterizations and relevant microphysical mechanisms. *Atmospheric Chemistry and Physics*, *19*(13), 8407–8424. <https://doi.org/10.5194/acp-19-8407-2019>
- Zinke, J., Salter, M., Leck, C., Lawler, M. J., Porter, G., Adams, M., et al. (2021). The development of a miniaturised balloon-borne cloud water sampler and its first deployment in the high Arctic. *Tellus B: Chemical and Physical Meteorology*. <https://doi.org/10.1080/16000889.2021.1915614>